

# Viable wormhole solution in Bopp–Podolsky electrodynamics

D. A. Frizo,<sup>1,\*</sup> C. A. M. de Melo,<sup>2,†</sup> L. G. Medeiros,<sup>3,‡</sup> and Juliano C. S. Neves<sup>2,§</sup>

<sup>1</sup>*Centro de Matemática, Computação e Cognição, Universidade Federal do ABC,  
Avenida dos Estados 5001, CEP 09210-580, Santo André, SP, Brazil*

<sup>2</sup>*Instituto de Ciência e Tecnologia, Universidade Federal de Alenas,*

*Rodovia José Aurélio Vilela, 11999, CEP 37715-400 Poços de Caldas, MG, Brazil*

<sup>3</sup>*Escola de Ciência e Tecnologia, Universidade Federal do Rio Grande do Norte,  
Campus Universitário, s/n-Lagoa Nova, Natal, RNCEP 59078-970, Brazil*

Following a recent approach in which the gravitational field equations in curved spacetimes were presented in the Bopp–Podolsky electrodynamics, we obtained an approximate and spherically symmetric wormhole solution in this context. The calculations were carried out up to the linear approximation in both the spacetime geometry and the radial electric field. The solution presents a new parameter that comes from the Lagrangian of the model. Such a parameter was constrained by using the shadow radius of Sagittarius A\*, recently revealed by the Event Horizon Telescope Collaboration. Remarkably, the wormhole presented here is viable when its shadow is compared to the Sagittarius A\* shadow.

Keywords: Wormhole, Electrodynamics, No-Hair Conjecture, Shadow

## I. INTRODUCTION

The Bopp–Podolsky electrodynamics [1, 2] is an extension of Maxwell’s theory in which a new second-order derivative of the gauge field is present in the Lagrangian, leading then to high-order field equations with fourth-order terms. As is well known, high-order theories in this context contain instabilities (like ghost instabilities). However, the Bopp–Podolsky electrodynamics is able to avoid this situation by means of the concept of Lagrange anchor [3]. Among the reasons to work on the Bopp–Podolsky model is its capability to preserve the linearity of the field equations being the only second-order gauge theory for the  $U(1)$  group that accomplishes that [4]. Moreover, in  $3+1$  dimensions (flat spacetime), the Bopp–Podolsky term in the Lagrangian can also be conceived of as an effective term coming from quantum corrections to the photon action in the low-energy regime [5].

Specific studies on the Bopp–Podolsky context have been done focusing, for example, on self-interaction [6, 7], dark energy [8], massive photons in cosmology [9] and spherically symmetric black holes [10]. In this work, we built an approximate solution with spherical symmetry extending the results of Ref. [10]. But contrary to the mentioned article [10], in which the spacetime geometry was studied without an analytic expression for the geometry, here we present a first-order approximation in order to obtain an explicit wormhole metric in Bopp–Podolsky electrodynamics. Such as in Cuzinatto et al. [10], our approximate wormhole solution also violates both the null (NEC) and the weak energy (WEC) conditions (energy conditions violations are important consequences in research areas like regular black holes [11] and bouncing cosmologies [12, 13] in today’s physics). In wormhole physics, violations of energy conditions at the wormhole throat are commonly reported [14–21]. Like the spacetime metric in the mentioned work [10], our solution also brings out the coupling constant  $b$ . In the mentioned article, because of  $b$ , the authors say their solution would not be in agreement with the no-hair conjecture.

The no-hair conjecture/theorem [22–24] states that black holes are fully described by just three parameters: mass, charge and spin. Contrary to Cuzinatto et al. [10], we do not interpret the new parameter  $b$  as some sort of hair. Besides, we claim that the solution of Ref. [10] is not a black hole, but a wormhole solution. Even so, a useful task is indicating constraints on the new parameter  $b$  unfolded by our approximate metric.

In this regard, we compare the shadow angular diameter or radius of the spacetime metric obtained here with the recent image of the Sagittarius A\* (Sgr A\*) shadow released by the Event Horizon Telescope (EHT) [25, 26]. Black hole and wormhole shadows have been a seminal research area since the very first shadow revealed by the EHT, the M87\* shadow [27, 28]. Two shadow parameters for constraining general relativity and modified theories of gravity have been adopted recently in the literature, namely the shadow angular diameter  $d_{\text{sh}}$  [29–34] and the

---

\*Electronic address: diego.frizo@ufabc.edu.br

†Electronic address: cassius.melo@unifal-mg.edu.br

‡Electronic address: leogmedeiros@gmail.com

§Electronic address: juliano.c.s.neves@gmail.com

shadow deviation from circularity  $\Delta C$  [35–41], which is nonzero for rotating black holes and is zero for nonrotating ones, that is to say, the shadow of spherical black holes or wormholes is a perfect circle. In particular, for the Sgr A\* black hole (or wormhole), due to the more precise measurements of distance and mass, the EHT [26] used the shadow angular diameter in order to provide a new parameter to be compared to black hole or wormhole metric candidates, whether in the general relativity context or in modified theories of gravity. From the shadow angular diameter, the new parameter called deviation from the Schwarzschild metric ( $\delta$ ) arises from the black hole mass-to-distance ratio and has been adopted, for example, in the pretty complete review on alternative theories of gravity and spherically symmetric black hole and wormhole metrics carried out by Vagnozzi et al. [31]. According to the authors of the mentioned review, the deviation from the Schwarzschild metric is, for example, a very good parameter to constraint spherical and “hairy” black holes, and wormholes by using the shadow of Sgr A\*. That is the reason why we are going to follow the approach presented in Ref. [31] in order to indicate that the metric obtained here is viable, i.e., for a range of parameters (mass, charge and coupling constant of the model), the spherically symmetric wormhole in the Bopp–Podolsky electrodynamics with the same mass of Sgr A\* is able to produce a shadow similar to that one captured by the EHT.

This article is structured as follows: in Sec. II the action, the electric field equations (also called Podolsky equations) and the gravitational field equations are presented for the Bopp–Podolsky electrodynamics in curved spacetimes. Both the gravitational and the electric field equations are solved in the linear approximation in Sec. III. Sec. IV is an attempt at indicating that the approximate solution is viable from the observational point of view according to the Sgr A\* shadow. The final comments are in Sec. V. In this article, we are adopting the geometrized units, that is,  $G = c = 1$ , where  $G$  is the gravitational constant, and  $c$  is the speed of light in vacuum.

## II. THE BOPP–PODOLSKY ELECTRODYNAMICS FOR CURVED SPACETIMES

In this section, both the action and field equations for curved spacetimes in the Bopp–Podolsky electrodynamics are written and briefly commented. According to Cuzinatto et al. [10], the Lagrangian in curved spacetimes for the Bopp–Podolsky electrodynamics is described by two new independent and invariant terms beyond the usual Maxwell term. The Lagrangian in this context is: (i) invariant under Lorentz transformations, (ii) gauge invariant under the  $U(1)$  symmetry group, (iii) quadratic in the gauge field and its derivatives, and (iv) dependent on the gauge field and its first two derivatives. As will see, the two new invariant terms in the Lagrangian are either minimally or nonminimally coupled to gravity. Assuming then this four conditions, the Bopp–Podolsky electrodynamics for curved spacetimes is described by the following Lagrangian:

$$\mathcal{L}_m = -\frac{1}{4}F^{\alpha\beta}F_{\alpha\beta} + \frac{(a^2 + 2b^2)}{2}\nabla_\beta F^{\alpha\beta}\nabla_\gamma F_\alpha{}^\gamma + b^2(R_{\sigma\beta}F^{\sigma\alpha}F_\alpha{}^\beta + R_{\alpha\sigma\beta\gamma}F^{\sigma\gamma}F^{\alpha\beta}), \quad (1)$$

where  $F_{\mu\nu} = \nabla_\mu A_\nu - \nabla_\nu A_\mu$  is the field strength,  $\nabla_\mu$  is the covariant derivative,  $a$  and  $b$  are coupling constants,  $R_{\mu\nu}$  is the Ricci tensor, and  $R_{\alpha\beta\gamma\delta}$  is the Riemann tensor.

By using the so-called Einstein–Hilbert action plus the term coming from the Bopp–Podolsky electrodynamics, namely

$$S = \frac{1}{16\pi} \int d^4x \sqrt{-g} (-R + 4\mathcal{L}_m), \quad (2)$$

in which  $g$  is the metric determinant,  $R$  is the Ricci scalar, and  $\mathcal{L}_m$  is given by Eq. (1), we are able to obtain the gravitational field equations and the equations for the gauge field, also called Bopp–Podolsky equations. In this regard, by varying the action (2) with respect to the metric field  $g_{\mu\nu}$ , one has the corresponding gravitational field equations:

$$R_{\mu\nu} - \frac{1}{2}g_{\mu\nu}R = 8\pi(T_{\mu\nu}^M + T_{\mu\nu}^a + T_{\mu\nu}^b), \quad (3)$$

where the components of the energy-momentum tensor are given by

$$T_{\mu\nu}^M = \frac{1}{4\pi} \left[ F_{\mu\sigma}F^\sigma{}_\nu + g_{\mu\nu} \frac{1}{4}F^{\alpha\beta}F_{\alpha\beta} \right], \quad (4)$$

$$T_{\mu\nu}^a = \frac{a^2}{4\pi} \left[ g_{\mu\nu}F_\beta{}^\gamma\nabla_\gamma K^\beta + \frac{g_{\mu\nu}}{2}K^\beta K_\beta + 2F_{(\mu}{}^\alpha\nabla_{\nu)}K_\alpha - 2F_{(\mu}{}^\alpha\nabla_\alpha K_{\nu)} - K_\mu K_\nu \right], \quad (5)$$

$$T_{\mu\nu}^b = \frac{b^2}{2\pi} \left[ -\frac{1}{4}g_{\mu\nu}\nabla^\beta F^{\alpha\gamma}\nabla_\beta F_{\alpha\gamma} + F_{(\mu}{}^\gamma\nabla_{\nu)}^\beta\nabla_\beta F_{\nu)\gamma} + F_{\gamma(\mu}\nabla_\beta\nabla_{\nu)}F^{\beta\gamma} - \nabla_\beta(F_\gamma{}^\beta\nabla_{(\mu}F_{\nu)}{}^\gamma) \right]. \quad (6)$$

The notation (...) indicates symmetrization with respect to the indexes inside the brackets.

On the other hand, by varying the action (2) with respect to the field  $A_\mu$ , we have the Bopp–Podolsky equations for curved spacetimes, namely

$$\nabla_\nu [F^{\mu\nu} - (a^2 + 2b^2) H^{\mu\nu} + 2b^2 S^{\mu\nu}] = 0, \quad (7)$$

where

$$H^{\mu\nu} \equiv \nabla^\mu K^\nu - \nabla^\nu K^\mu, \quad (8)$$

$$S^{\mu\nu} \equiv F^{\mu\sigma} R_\sigma{}^\nu - F^{\nu\sigma} R_\sigma{}^\mu + 2R^\mu{}_\sigma{}^\nu F^{\beta\sigma}, \quad (9)$$

with  $K^\mu \equiv \nabla_\gamma F^{\mu\gamma}$ . It is worth pointing out that any valid solution in the Bopp–Podolsky context must be solution of either field equations, whether the gravitational field equations (3) or the Bopp–Podolsky equations (7).

In Ref. [10], by using the Bekenstein method, even without an explicit form for the spacetime metric, it was shown that for  $b = 0$  the exterior solution of a spherically symmetric black hole is the Reissner–Nordström solution, i.e., the no-hair theorem is fully satisfied. However, the same authors claimed that hairy black hole solutions would be possible only if both  $b \neq 0$  and  $\frac{dq_{00}}{dr} \geq 0$ , where  $r$  is the radial coordinate. In the next section, using a perturbative approach, we then show explicitly that the  $b \neq 0$  case generates instead a wormhole solution.

From the energy conservation perspective, the total energy-momentum tensor is conserved, i.e., given  $T_{\mu\nu} = T_{\mu\nu}^M + T_{\mu\nu}^a + T_{\mu\nu}^b$ , one has

$$\nabla_\nu T^{\mu\nu} = 0, \quad (10)$$

with the aid of the constraint provided by the Bopp–Podolsky equations (7). In particular, for the spherically symmetric *Ansatz* that we used in this study (independently of the metric terms) and a radial electric field, every component of Eq. (10) is identically zero, regardless the  $\mu = 1$  component. Such a component becomes zero by using the  $\mu = 1$  component of the Bopp–Podolsky equations.

### III. AN APPROXIMATE SOLUTION

#### A. The spacetime metric

When dealing with higher-order theories in which the coupling parameters are very small, the correct perturbative scheme is given by the singular perturbation theory [42, 43]. The influence of higher derivatives is important inside a boundary layer, whose size is proportional to the coupling constants coming from the higher-order derivatives, while outside that boundary the solution is asymptotically the nonperturbed solution, and the regular approach for obtaining approximate solutions is enough. In our case, the higher-order derivatives of the electric field are proportional to the parameters or coupling constants  $a$  and  $b$ . Since we are interested in the exterior solution, we are dealing with scale distances such that (in geometrized units)

$$a, b \ll r_+ \leq r < \infty, \quad (11)$$

where  $r_+$  is the radius of the external horizon, the usual event horizon radius, in a black hole solution. This implies that we are able to use only the regular perturbation theory throughout this article.

Having said that, we present here an approximate solution with spherical symmetry in the context indicated in Section II by using the regular perturbation theory. Due to the nonlinearity of the field equations (as for the metric components), approximate solutions are an alternative alongside the numerical approach. From the spherically symmetric *Ansatz* in the  $(t, r, \theta, \phi)$  coordinates, i.e.,

$$ds^2 = A(r)dt^2 - \frac{dr^2}{B(r)} - r^2 (d\theta^2 + \sin^2 \theta d\phi^2), \quad (12)$$

an approximate solution will be available if we assume

$$A(r) = A_0(r) + \epsilon A_1(r), \quad (13)$$

$$B(r) = B_0(r) + \epsilon B_1(r), \quad (14)$$

$$E(r) = E_0(r) + \epsilon E_1(r). \quad (15)$$

As we are looking for a small deviation from the Reissner–Nordström geometry, then we assume the following input for the metric and the radial electric field, i.e.,

$$A_0(r) = B_0(r) = 1 - \frac{2M}{r} + \frac{Q^2}{r^2} \quad \text{and} \quad E_0(r) = \frac{Q}{r^2}, \quad (16)$$

where  $\epsilon = \epsilon(a, b)$  is a small quantity, and we take the perturbations just to the linear order.

Another important input of the model is the field strength  $F_{\mu\nu}$ . From the small deviation of the Reissner–Nordström black hole in which we are interested, we assume that

$$F_{\mu\nu} = E(r) [\delta_\mu^1 \delta_\nu^0 - \delta_\mu^0 \delta_\nu^1]. \quad (17)$$

Thus, the system of equations provided by the gravitational field equations depends on just three functions:  $A(r)$ ,  $B(r)$  and  $E(r)$  or, in the perturbative approach that we adopt,  $A_1(r)$ ,  $B_1(r)$  and  $E_1(r)$ .

The field equations (3), by using the approximation (13)-(15) and the field strength (17), give us the following system of differential equations:

$$B_1'(r) + \left( \frac{Q^2 + F(r)}{rF(r)} \right) B_1(r) - \frac{Q^2}{rF(r)} A_1(r) + \frac{2Q}{r} E_1(r) - \frac{4b^2 Q^2}{\epsilon r^7} (7Q^2 + (3r - 10M)r) = 0, \quad (18)$$

$$A_1'(r) - \left( \frac{r^2 - F(r)}{rF(r)} \right) A_1(r) + \frac{r}{F(r)} B_1(r) + \frac{2Q}{r} E_1(r) - \frac{4b^2 Q^2}{\epsilon r^7} (Q^2 - (3r - 2M)r) = 0, \quad (19)$$

$$\begin{aligned} A_1''(r) + \left( \frac{Q^2 - Mr + F(r)}{rF(r)} \right) A_1'(r) + \left( \frac{r - M}{F(r)} \right) B_1'(r) - \frac{4Q}{r^2} E_1(r) + \left( 2 \frac{(r - M)(Mr - Q^2)}{rF(r)^2} \right) (A_1(r) - B_1(r)) \\ - \frac{16b^2 Q^2}{\epsilon r^8} (4Q^2 + (3r - 7M)r) = 0, \end{aligned} \quad (20)$$

with the operator ' playing the role of the derivative with respect to the radial coordinate, and

$$F(r) = Q^2 + (r - 2M)r. \quad (21)$$

An interesting point here is that by assuming the *Ansätze* (13)-(16), especially  $E_0(r)$ , all terms with  $a$  disappear in the field equations, because all terms coming from the invariant  $\nabla_\beta F^{\alpha\beta} \nabla_\gamma F_\alpha^\gamma$  are considered zero in the approximation made here. That is, such an invariant term in the Lagrangian, owing to the mentioned *Ansätze*, brings the factor  $(a^2 + 2b^2)\epsilon^2$ , which is approximately zero. Therefore, only the nonminimal terms will contribute with the perturbed equations, namely terms with  $b^2$ .

As we can see, we have three independent differential equations with three unknown functions:  $A_1(r)$ ,  $B_1(r)$  and  $E_1(r)$ . In this regard, the system indicated in Eqs. (18)-(20) is solvable, and by assuming that the sough-after geometry is a small deviation from the Reissner–Nordström spacetime, meaning that our solution is asymptotically flat, that is to say, the limits  $\lim_{r \rightarrow \infty} A_1(r) = \lim_{r \rightarrow \infty} B_1(r) = \lim_{r \rightarrow \infty} E_1(r) = 0$  are necessarily true, one has the following solution for the system of differential equations:

$$A_1(r) = \frac{2b^2 Q^2}{\epsilon r^4} \left( 1 - \frac{3M}{r} + \frac{9Q^2}{5r^2} \right), \quad (22)$$

$$B_1(r) = -\frac{2b^2 Q^2}{\epsilon r^4} \left( 2 - \frac{3M}{r} + \frac{6Q^2}{5r^2} \right), \quad (23)$$

$$E_1(r) = -\frac{b^2 Q}{\epsilon r^4} \left( \frac{8M}{r} - \frac{11Q^2}{r^2} \right). \quad (24)$$

From the above result, we see that when Eqs. (22)-(24) are substituted into Eq. (13)-(15), the real expansion parameter will be  $\frac{b}{r} \ll 1$  for a small deviation from the Reissner–Nordström spacetime. Then the parameter  $\epsilon$  is some sort of auxiliary parameter in the approach adopted here, something usual in standard procedures both in regular and singular perturbation theory (see Refs. [42, 43]). It disappears once one substitutes Eqs. (22)-(24) into Eqs. (13)-(15). In the end of the day, the small deviation from the standard geometry will be given by the coupling constant  $b$ . Thus,  $b$  is assumed to be a very small parameter.

It is worth pointing out that Eqs. (22)-(24) are exact solutions of the system (18)-(20), regardless the value of the radial coordinate  $r$ . Therefore, with Eqs. (22)-(23) substituted into the linear approximation (13)-(14), we arrive

then in the fully calculated geometry, which is written as

$$ds^2 = \left( 1 - \frac{2M}{r} + \frac{Q^2}{r^2} + \frac{2b^2Q^2}{r^4} - \frac{6Mb^2Q^2}{r^5} + \frac{18b^2Q^4}{5r^6} \right) dt^2 - \left( 1 - \frac{2M}{r} + \frac{Q^2}{r^2} - \frac{4b^2Q^2}{r^4} + \frac{6Mb^2Q^2}{r^5} - \frac{12b^2Q^4}{5r^6} \right)^{-1} dr^2 - r^2 (d\theta^2 + \sin^2\theta d\phi^2). \quad (25)$$

As is clear from the metric (25), by making  $b = 0$  the Reissner–Nordström geometry is restored. And contrary to the well-known black hole solutions with spherical symmetry in the general relativity context, the spacetime metric obtained here has  $A(r) \neq B(r)$ , which is something usual in modified theories of gravity.<sup>1</sup>

As we can read from Eq. (25), the metric presents a new parameter  $b$ , and this new parameter could be interpreted as hair. Then the no-hair conjecture would be refuted. Cuzinatto et al. [10] argue in favor of a hairy black hole in the Bopp–Podolsky context. But, as we mentioned, such authors argue without an explicit metric like ours. In this regard, we disagree that  $b$  would be a black hole parameter with the same status of mass, charge or spin. By conceiving of  $b$  as a constant of nature instead of a body property like mass or charge, the presence of  $b$  is not in disagreement with the no-hair conjecture. Following Cuzinatto et al. [10], the two conditions for a hairy and spherically symmetric black hole in Bopp–Podolsky electrodynamics, mentioned in Sec. II, namely  $b \neq 0$  and  $g'_{00} \geq 0$ , are fulfilled by the metric (25). But, according to our understanding, those conditions are not necessary conditions for generating hair in the context studied here. Moreover, as we will see, the metric (25) is a wormhole, not a black hole solution.

The radial electric field, from Eqs. (15) and (24), is now written as

$$E(r) = \frac{Q}{r^2} \left( 1 - \frac{8Mb^2}{r^3} + \frac{11b^2Q^2}{r^4} \right). \quad (26)$$

And, as expected, turning off  $b$  the usual electric field is obtained. For large values of  $r$ , the influence of  $b$  on the electric field is very tiny. In this range of the radial coordinate, the electric field is asymptotically the usual electric field for a point charge:  $E(r) \rightarrow E_0(r)$ . It is worth pointing out the weirdness of the new term that contains the mass parameter in Eq. (26), for it seems like the radial electric field was truly coupled to the spacetime geometry.

As we said, the metric (25) is an approximate solution with spherical symmetry in the Bopp–Podolsky electrodynamics. We will see that the solution (25) captures the same features pointed out in the analysis carried out by Cuzinatto et al. [10], whose study is made from the Bekenstein method, even without a final expression for the spacetime metric. As we can read from Eq. (25), the spacetime geometry is asymptotically flat, that is, the flatness condition

$$\lim_{r \rightarrow \infty} A(r) = \lim_{r \rightarrow \infty} B(r) = 1 \quad (27)$$

is achieved. Also it is worth emphasizing that the metric (25) is solution of the Bopp–Podolsky equation (7) in its approximate version, in which high-order terms of  $\epsilon$  were also ruled out.

## B. The spacetime structure

By spacetime structure we mean the localization of horizons and, of course, type of infinities. As we saw in Eq. (27), the proposed solution is, like the Reissner–Nordström spacetime, asymptotically flat, i.e., it has the same infinite configuration or type of infinities of that well-known solution of Einstein's equations. But, supposedly, the metric (25) presents a larger number of horizons. The localization of horizons in spacetimes like (12) is given by the equation  $g^{rr} = B(r) = 0$  in cases when  $A(r)$  and  $B(r)$  share the same roots. Typically, for  $M > Q$ , the function  $B(r)$  would have at most three positive and real roots, which would be horizons: two inner horizons (being the larger one the usual inner horizon of the Reissner–Nordström spacetime,  $r_-$ ) and one outer horizon, which is indicated as  $r_+$  and would play the role of the event horizon. However, as we said, due to the perturbative approach and the application of spacetime (25) to the shadow phenomenon, we are interested in the interval  $r \geq r_+$ , which is regular.

However, the condition  $A(r) \neq B(r)$  could raise questions about the metric signature and the existence of an event horizon. As we can read from Eq. (25), we adopt the metric signature  $(+, -, -, -)$ , also called Lorentzian signature. But from values of  $r \leq r_+$ , owing to the fact that  $A(r) \neq B(r)$ , we would have a non-Lorentzian signature because the outermost root of  $A(r)$ , namely  $r_0$ , would not coincide with  $r_+$  (see Fig. 1), that is,  $A(r)$  and  $B(r)$  do not share

---

<sup>1</sup> In other contexts beyond general relativity, like braneworld, the condition  $A(r) \neq B(r)$  is quite common. See Refs. [19, 20].

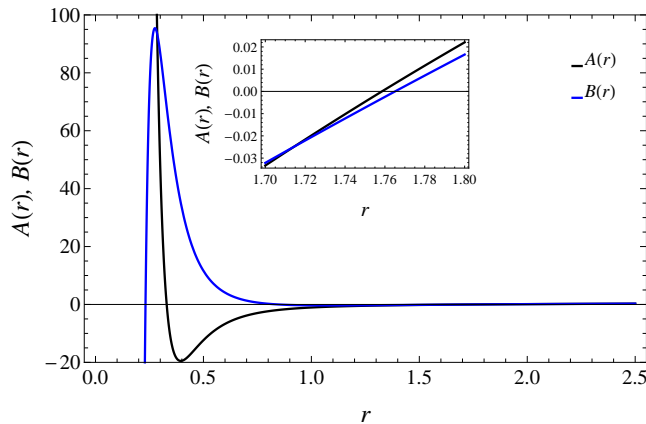


Figure 1: The metric functions  $A(r)$  and  $B(r)$  given by Eq. (25). The asymptotic behavior is indicated. Also, one sees that the functions  $A(r)$  and  $B(r)$  present different zeros. This is one of the reasons why we interpret such a solution as a wormhole solution. In this graphic, one adopts  $M = 1$ ,  $Q = 0.7$  and  $b = 0.7$ .

the same root. Even worse, we would not have an event horizon, for the surface  $r = r_+$  would not be a null surface. Then the line element  $ds$ , for constant  $r, \theta$  and  $\phi$ , would not be zero at  $r_+$ . Here, we see a limitation of the chart  $(t, r, \theta, \phi)$  for describing our spacetime.

In order to overcome this situation, we interpret the solution (25) as a wormhole solution. Then the radial coordinate is valid just for  $r > r_+ = r_{\text{thr}}$ . Now  $r = r_{\text{thr}}$  indicates the wormhole throat localization in spacetime. Thus, instead of the event horizon,  $g^{rr} = B(r) = 0$  provides an extremum of the radial coordinate,  $r = r_{\text{thr}}$ . Consequently, the functions  $A(r)$  and  $B(r)$  are positive-definite functions for  $r > r_{\text{thr}}$ , and both the metric is Lorentzian and the chart  $(t, r, \theta, \phi)$  is still valid for  $r_{\text{thr}} < r < \infty$ . Following Refs.[14, 19, 20], one defines then the proper length  $\ell(r)$  as the new radial function, i.e.,

$$\frac{d\ell(r)}{dr} = \frac{1}{\sqrt{B(r)}}. \quad (28)$$

With the new coordinate  $\ell(r)$ , by assuming an appropriate integration constant in Eq. (28), the region  $r_{\text{thr}} < r < \infty$  is mapped into  $0 < \ell < \infty$ , and an analytic extension beyond  $r = r_{\text{thr}}$  is viable. Thus, we have two distant regions being connected by the wormhole hole throat at  $\ell = 0$ . It is worth pointing out that the wormhole solution proposed here is traversable, that is, it has no event horizon. Moreover, the spacetime metric after the analytic extension  $-\infty < \ell < \infty$  is regular, because from the Kretschmann scalar calculation the metric (25) shows divergence at  $A(r_0) = 0$ , in which  $r_0 < r_{\text{thr}}$ . That is,  $r = r_0$  is not part of spacetime anymore, thus the metric is regular.

As we will see in the next subsection, the interpretation of (25) as a wormhole solution is in agreement with the violation of the NEC and WEC, as several studies found out in wormhole geometries.

### C. Energy conditions

As mentioned in Cuzinatto et al. [10], where an analysis in the context adopted here was made without a final form for the spacetime metric, a spherically symmetric solution in the Bopp–Podolsky electrodynamics is able to violate energy conditions. In particular, as we said, both the NEC and the WEC are violated. From the total energy-momentum tensor given by  $T_{\mu\nu} = T_{\mu\nu}^M + T_{\mu\nu}^a + T_{\mu\nu}^b$ , one has

$$T_{\nu}^{\mu} = \begin{pmatrix} \rho(r) & & & \\ & -p_1(r) & & \\ & & -p_2(r) & \\ & & & -p_3(r) \end{pmatrix}. \quad (29)$$

For an energy-momentum tensor written as the diagonal matrix like Eq. (29), the WEC states that  $\rho(r) > 0$  and, at the same time, the condition  $\rho + p_i \geq 0$  (for every  $i = 1, 2, 3$ ) should also be satisfied. That is not the case for the

metric (25). As for the energy density, for the metric (25) in the Bopp–Podolsky electrodynamics, we have

$$\rho(r) = \frac{Q^2}{8\pi r^4} \left( 1 - \frac{12b^2}{r^2} A_0(r) \right) > 0. \quad (30)$$

From the fact that  $A_0(r) > 0$  for  $r > r_{\text{thr}}$ , being the second term on the right side of Eq. (30)  $\ll 1$ , we can read that the energy density  $\rho(r)$  is positive definite surely for  $r > r_{\text{thr}}$ , which is the range of validity of the perturbative approach adopted by us.

On the other hand, as the condition  $\rho + p_i \geq 0$  (for every  $i = 1, 2, 3$ ) is a true statement of either energy conditions, thus both the NEC and WEC are not satisfied. In particular, for  $i = 1$ , this condition reads

$$\rho(r) + p_1(r) = -\frac{3b^2 Q^2}{\pi r^6} A_0(r), \quad (31)$$

which vanishes for  $b = 0$  and is negative for  $r > r_{\text{thr}}$ , that is to say, the wormhole obtained here is not in agreement with the NEC and WEC. Therefore, as a possible interpretation, the model introduced in Section II could be translated into an exotic matter that does not satisfy energy conditions and provides a wormhole throat. In nonlinear electrodynamics, for example, according to Ref. [44], violations of energy conditions could lead to tachyons or signals faster than light in vacuum.

It is worth pointing out an interesting result in Ref. [10] concerning the energy-momentum tensor. According to the mentioned article, the trace of  $T_{\mu\nu}$ , which is associated with the total energy of the system, would be finite for  $r = r_{\text{thr}}$  independently of  $b$ . As the trace of the energy-momentum tensor is  $T^\mu_\mu = T \sim 1/A(r)^2$ , one has a finite value of  $T$  when  $r = r_{\text{thr}}$ .

## IV. THE WORMHOLE SHADOW

### A. Radius of the shadow

As the wormhole geometry (25) has spherical symmetry, the shadow silhouette is circular. In general, shadows are deformed by the black hole or wormhole spin, which is not our case here. According to EHT [27, 28], the M87\* shadow presents a small deviation from the perfect circle, a deviation from circularity  $\Delta C \lesssim 10\%$ , indicating then that M87\* is spinning. But due to the less precise data from the Sgr A\* image (because of intense variability of its surroundings and the sparse coverage of the observations in 2017 [26]), the most precise parameter to be studied is the shadow angular size or angular diameter  $d_{\text{sh}}$ .

Black hole and wormhole shadows are generated by the so-called photon sphere, which is a region delimited by unstable photon orbits. Part of photons traveling in these orbits falls into the hole, and part of them could escape to an observer like us. For supermassive objects like M87\* and Sgr A\*, the shadow, a brightness depression, is surrounded by a bright and thick ring of emission. According to EHT [26], under certain circumstances, the size of the emission ring could be an approximate value for the shadow.

The shadow silhouette is given by the photon sphere, and, according to Perlick and Tsupko [45], from an interesting geometric argumentation, metrics like (12) present a photon sphere whose radius is given by the following equation:

$$A(r_{\text{ph}}) - \frac{1}{2} r_{\text{ph}} A'(r_{\text{ph}}) = 0, \quad (32)$$

where  $r_{\text{ph}}$  is the photon sphere radius. Following the mentioned article, then the shadow radius  $r_{\text{sh}}$  reads

$$r_{\text{sh}} = \frac{r_{\text{ph}}}{\sqrt{A(r_{\text{ph}})}}. \quad (33)$$

As expected, the shadow radius is not equal to the photon sphere radius. The gravitational lensing increases the shadow radius when it is observed from a distance. Due to the high-order polynomial expression for calculating  $r_{\text{ph}}$ , we will omit the analytic result here. But for our purpose, the main information comes from the shadow radius, where its dependence on the coupling constant is shown in Fig. 2. As we can read from that figure, the coupling constant decreases the shadow radius. This could be a point in favor of our metric, for the EHT image disfavors alternative black holes and wormholes that generate larger shadows than the Schwarzschild black hole. However, as the EHT points out [26], the most favorite candidate for the Sgr A\* image is the Kerr metric, that is, the observed image size is within  $\sim 10\%$  of the Kerr geometry predictions.

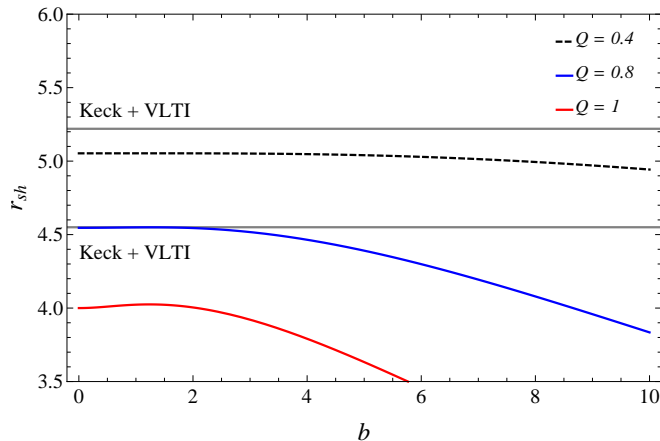


Figure 2: The dependence of the shadow radius  $r_{\text{sh}}$  on both the charge parameter  $Q$  and coupling constant  $b$ . Exaggerated values of  $b$  were chosen in order to better illustrate their effects on the shadow radius. The parameter  $b$  decreases the shadow radius. The horizontal lines indicate the viable  $1\sigma$  interval of the shadow radius, given by Eq. (36), in agreement with the Sgr A\* shadow radius using the mass-to-distance ratio from Keck + VLTI. In this graphic, we adopt the geometrized units and  $M = 1$ .

Table I: Mass, in solar masses, and distance, in parsec, of Sgr A\* according to Keck observatory and VLTI.

Survey	$M$ ( $10^6 M_{\odot}$ )	$D$ (kpc)
Keck <sup>a</sup>	$3.975 \pm 0.058$	$7.959 \pm 0.059$
VLTI <sup>b</sup>	$4.297 \pm 0.012$	$8.277 \pm 0.009$

<sup>a</sup>See Ref. [46].

<sup>b</sup>See Ref. [47].

## B. Constraining the wormhole parameters using the Sgr A\* shadow

As we said in Introduction, in order to compare the geometry (25) to the Sgr A\* black hole, the crucial parameter here is the deviation from the Schwarzschild metric  $\delta$ . As the Sgr A\* spin is still unknown, geometries with spherical symmetry are not ruled out for describing our galactic central compact object. A recent estimation for the dimensionless spin parameter for Sgr A\* is  $a_* \lesssim 0.1$  [48, 49], where  $0 < a_* < 1$  for spinning black holes/wormholes, that is to say, arguably our central object is spinning slowly. Thus, describing Sgr A\* approximately as a static black hole (like the Schwarzschild black hole or a deviation from the Schwarzschild geometry as a wormhole) is not out of question. Therefore, according to EHT [26], the deviation from the Schwarzschild metric is conceived of as

$$\delta = \frac{d_{\text{sh}}}{d_{\text{Sch}}} - 1, \quad (34)$$

where  $d_{\text{sh}} = 48.7 \pm 7.0 \mu\text{as}$  is the shadow angular diameter of Sgr A\* (measured by the EHT),  $d_{\text{Sch}} = 6\sqrt{3}\theta_g$  is the angular diameter for the Schwarzschild black hole in the small angle approximation, and  $\theta_g$  is called angular gravitational radius, which is given by  $\theta_g = GM/Dc^2$  where  $M$  is the black hole or wormhole mass, and  $D$  is its distance from us ( $G$  and  $c$  are the gravitational constant and the speed of light in vacuum, which were set to 1 in the geometrized unit system adopted in this article). The most precise values for mass and distance of Sgr A\*, even adopted by the EHT, were obtained by the Keck observatory and VLTI (Very Large Telescope Interferometer) (see Table I). Both values provide the mass-to-distance ratio of our central black hole/wormhole. With those parameters for Sgr A\*, the deviation given by Eq. (34) is  $\delta = -0.04_{-0.10}^{+0.09}$  for the Keck observatory, and  $\delta = -0.08_{-0.09}^{+0.09}$  for the VLTI.

Following Vagnozzi et al. [31], the idea is calculating a valid range for the shadow radius of a wormhole like our spacetime (25) using the deviation  $\delta$ . Spherically symmetric solutions—like the Reissner–Nordström black hole, regular black holes, naked singularities or wormholes and black holes in several contexts like  $f(R)$  gravity, braneworld, Horndeski model, bumblebee gravity, loop quantum gravity—were constrained by the authors. For that purpose, Vagnozzi et al. [31] obtained a combined value of  $\delta$  using the two surveys, Keck and VLTI, considering them

independent results. That procedure gives us

$$\delta \simeq -0.060 \pm 0.065, \quad (35)$$

which leads to the following  $1\sigma$  constraint for the shadow radius as a deviation from the Schwarzschild metric:

$$\begin{aligned} 3\sqrt{3}(1 - 0.125) \lesssim \frac{r_{\text{sh}}}{M} \lesssim 3\sqrt{3}(1 + 0.005), \\ 4.55M \lesssim r_{\text{sh}} \lesssim 5.22M. \end{aligned} \quad (36)$$

It is worth emphasizing that  $r_{\text{sh}}$  is the shadow radius, not the angular radius. Having said that, the range above constrains alternative geometries (like ours) allowed by the observations. In this regard, Fig. 2 indicates upper bounds on the charge parameter,  $Q \lesssim 0.8M$ , and on the coupling constant, namely  $b \lesssim 2M$ . We conclude then that our solution is still viable, for it was designed for  $b \ll 2M$  according to the perturbative approach.

## V. FINAL COMMENTS

In this article, we built an approximate wormhole solution with spherical symmetry in Bopp–Podolsky electrodynamics. The final form of the spacetime metric shows a third parameter, alongside the mass and charge parameters, which comes from the action of the model and is conceived of as the nonminimal coupling constant. Because of this parameter, the modified radial electric field violates massively both the NEC and WEC at the wormhole throat.

In the final part of this work, data from the EHT Collaboration and from the Keck and VLTI observatories were adopted in order to compare the wormhole obtained here with Sgr A\*, the central compact object in the Milky Way galaxy. These data constrain the range of validity of the shadow radius, when Sgr A\* is considered as a small deviation from the Schwarzschild black hole. The new parameter in the metric, the nonminimal coupling constant, which was constrained from the Sgr A\* shadow, makes the radius of the wormhole shadow smaller when it is compared with the Schwarzschild shadow, something in agreement with the EHT report. As we pointed out, the metric obtained is viable using the valid range of the shadow radius of Sgr A\*. In this sense, Sgr A\* could still be described as a wormhole.

## Acknowledgments

LGM acknowledges CNPq-Brazil (Grant No. 308380/2019-3) for the partial financial support. JCSN thanks the ICT-UNIFAL for the kind hospitality. We thank two anonymous referees for comments and valuable suggestions.

- 
- [1] F. Bopp, Eine lineare Theorie des Elektrons, *Ann. Phys.* **430**, 345 (1940).
  - [2] B. Podolsky, A Generalized Electrodynamics Part I-Non-Quantum, *Phys. Rev.* **62**, 68-71 (1942).
  - [3] D. S. Kaparulin, S. L. Lyakhovich and A. A. Sharapov, Classical and quantum stability of higher-derivative dynamics, *Eur. Phys. J. C* **74**, no.10, 3072 (2014).
  - [4] R. R. Cuzinatto, C. A. M. de Melo and P. J. Pompeia, Second order gauge theory, *Annals Phys.* **322**, 1211-1232 (2007).
  - [5] L. H. C. Borges, F. A. Barone, C. A. M. de Melo and F. E. Barone, Higher order derivative operators as quantum corrections, *Nucl. Phys. B* **944**, 114634 (2019).
  - [6] A. E. Zayats, Self-interaction in the Bopp-Podolsky electrodynamics: Can the observable mass of a charged particle depend on its acceleration?, *Annals Phys.* **342**, 11-20 (2014).
  - [7] A. E. Zayats, Self-interaction in Bopp-Podolsky electrodynamics: Spacetimes with angular defects, *Phys. Rev. D* **94**, no.10, 105026 (2016).
  - [8] Z. Haghani, T. Harko, H. R. Sepangi and S. Shahidi, Vector dark energy models with quadratic terms in the Maxwell tensor derivatives, *Eur. Phys. J. C* **77**, no.3, 137 (2017).
  - [9] R. R. Cuzinatto, E. M. de Moraes, L. G. Medeiros, C. Naldoni de Souza and B. M. Pimentel, de Broglie-Proca and Bopp-Podolsky massive photon gases in cosmology, *EPL* **118**, no.1, 19001 (2017).
  - [10] R. R. Cuzinatto, C. A. M. de Melo, L. G. Medeiros, B. M. Pimentel and P. J. Pompeia, Bopp–Podolsky black holes and the no-hair theorem, *Eur. Phys. J. C* **78**, no.1, 43 (2018).
  - [11] J. C. S. Neves and A. Saa, Regular rotating black holes and the weak energy condition, *Phys. Lett. B* **734**, 44-48 (2014).
  - [12] M. Novello and S. E. P. Bergliaffa, Bouncing Cosmologies, *Phys. Rept.* **463**, 127-213 (2008).
  - [13] R. Brandenberger and P. Peter, Bouncing Cosmologies: Progress and Problems, *Found. Phys.* **47**, no.6, 797-850 (2017).

- [14] M. S. Morris and K. S. Thorne, Wormholes in space-time and their use for interstellar travel: A tool for teaching general relativity, *Am. J. Phys.* **56**, 395-412 (1988).
- [15] M. Visser, S. Kar and N. Dadhich, Traversable wormholes with arbitrarily small energy condition violations, *Phys. Rev. Lett.* **90**, 201102 (2003).
- [16] J. P. S. Lemos, F. S. N. Lobo and S. Quinet de Oliveira, Morris-Thorne wormholes with a cosmological constant, *Phys. Rev. D* **68**, 064004 (2003).
- [17] K. A. Bronnikov and S. W. Kim, Possible wormholes in a brane world, *Phys. Rev. D* **67**, 064027 (2003)
- [18] F. S. N. Lobo, Phantom energy traversable wormholes, *Phys. Rev. D* **71**, 084011 (2005).
- [19] C. Molina and J. C. S. Neves, Black holes and wormholes in AdS branes, *Phys. Rev. D* **82**, 044029 (2010).
- [20] C. Molina and J. C. S. Neves, Wormholes in de Sitter branes, *Phys. Rev. D* **86**, 024015 (2012).
- [21] C. R. Muniz and R. V. Maluf, A class of traversable wormholes in the Starobinsky-like  $f(R)$  gravity with anisotropic dark matter, *Annals Phys.* **446**, 169129 (2022).
- [22] W. Israel, Event horizons in static vacuum space-times, *Phys. Rev.* **164**, 1776-1779 (1967)
- [23] W. Israel, Event horizons in static electrovac space-times, *Commun. Math. Phys.* **8**, 245-260 (1968)
- [24] B. Carter, Axisymmetric Black Hole Has Only Two Degrees of Freedom, *Phys. Rev. Lett.* **26**, 331-333 (1971).
- [25] K. Akiyama *et al.* [Event Horizon Telescope], First Sagittarius A\* Event Horizon Telescope Results. I. The Shadow of the Supermassive Black Hole in the Center of the Milky Way, *Astrophys. J. Lett.* **930**, no.2, L12 (2022).
- [26] K. Akiyama *et al.* [Event Horizon Telescope], First Sagittarius A\* Event Horizon Telescope Results. VI. Testing the Black Hole Metric, *Astrophys. J. Lett.* **930**, no.2, L17 (2022).
- [27] K. Akiyama *et al.* [Event Horizon Telescope], First M87 Event Horizon Telescope Results. I. The Shadow of the Supermassive Black Hole, *Astrophys. J. Lett.* **875**, L1 (2019).
- [28] K. Akiyama *et al.* [Event Horizon Telescope], First M87 Event Horizon Telescope Results. VI. The Shadow and Mass of the Central Black Hole, *Astrophys. J. Lett.* **875**, no.1, L6 (2019).
- [29] M. Khodadi, A. Allahyari, S. Vagnozzi and D. F. Mota, Black holes with scalar hair in light of the Event Horizon Telescope, *JCAP* **09**, 026 (2020).
- [30] R. V. Maluf and J. C. S. Neves, Black holes with a cosmological constant in bumblebee gravity, *Phys. Rev. D* **103**, no.4, 044002 (2021).
- [31] S. Vagnozzi, R. Roy, Y. D. Tsai, L. Visinelli, M. Afrin, A. Allahyari, P. Bambhaniya, D. Dey, S. G. Ghosh and P. S. Joshi, *et al.* Horizon-scale tests of gravity theories and fundamental physics from the Event Horizon Telescope image of Sagittarius A\*, arXiv:2205.07787.
- [32] M. Khodadi and G. Lambiase, Probing Lorentz symmetry violation using the first image of Sagittarius A\*: Constraints on standard-model extension coefficients, *Phys. Rev. D* **106**, no.10, 104050 (2022).
- [33] R. Kumar Walia, S. G. Ghosh and S. D. Maharaj, Testing Rotating Regular Metrics with EHT Results of Sgr A\*, *Astrophys. J.* **939**, no.2, 77 (2022).
- [34] M. Afrin, S. Vagnozzi and S. G. Ghosh, Tests of Loop Quantum Gravity from the Event Horizon Telescope Results of Sgr A\*, *Astrophys. J.* **944**, no.2, 149 (2023).
- [35] C. Bambi, K. Freese, S. Vagnozzi and L. Visinelli, Testing the rotational nature of the supermassive object M87\* from the circularity and size of its first image, *Phys. Rev. D* **100**, no.4, 044057 (2019).
- [36] J. C. S. Neves, Upper bound on the GUP parameter using the black hole shadow, *Eur. Phys. J. C* **80**, no.4, 343 (2020).
- [37] J. C. S. Neves, Constraining the tidal charge of brane black holes using their shadows, *Eur. Phys. J. C* **80**, no.8, 717 (2020).
- [38] R. Kumar and S. G. Ghosh, Photon ring structure of rotating regular black holes and no-horizon spacetimes, *Class. Quant. Grav.* **38**, no.8, 8 (2021).
- [39] I. Banerjee, S. Chakraborty and S. SenGupta, Silhouette of M87\*: A New Window to Peek into the World of Hidden Dimensions, *Phys. Rev. D* **101**, no.4, 041301 (2020).
- [40] M. Khodadi, G. Lambiase and D. F. Mota, No-hair theorem in the wake of Event Horizon Telescope, *JCAP* **09**, 028 (2021).
- [41] R. Kumar, A. Kumar and S. G. Ghosh, Testing Rotating Regular Metrics as Candidates for Astrophysical Black Holes, *Astrophys. J.* **896**, no.1, 89 (2020).
- [42] R. Johnson, *Singular Perturbation Theory: Techniques with Applications to Engineering* (Springer, New York, 2004).
- [43] M. H. Holmes, *Introduction to Perturbation Methods* (Springer, New York, 2012).
- [44] A. E. Shabad and V. V. Usov, Effective Lagrangian in nonlinear electrodynamics and its properties of causality and unitarity, *Phys. Rev. D* **83**, 105006 (2011).
- [45] V. Perlick and O. Y. Tsupko, Calculating black hole shadows: Review of analytical studies, *Phys. Rept.* **947**, 1-39 (2022).
- [46] T. Do, A. Hees, A. Ghez, G. D. Martinez, D. S. Chu, S. Jia, S. Sakai, J. R. Lu, A. K. Gautam and K. K. O'Neil, *et al.* Relativistic redshift of the star S0-2 orbiting the Galactic center supermassive black hole, *Science* **365**, no.6454, 664-668 (2019).
- [47] R. Abuter *et al.* [GRAVITY], Mass distribution in the Galactic Center based on interferometric astrometry of multiple stellar orbits, *Astron. Astrophys.* **657**, L12 (2022).
- [48] G. Fragione and A. Loeb, An upper limit on the spin of SgrA\* based on stellar orbits in its vicinity, *Astrophys. J. Lett.* **901**, no.2, L32 (2020).
- [49] G. Fragione and A. Loeb, Implication of Spin Constraints by the Event Horizon Telescope on Stellar Orbits in the Galactic Center, *Astrophys. J. Lett.* **932**, no.2, L17 (2022).